Journal of Thermal Analysis and Calorimetry, Vol. 83 (2006) 1, 87–90

ENTHALPY RELAXATION AND FRAGILITY IN POLYCHLORINATED BIPHENYLS

C. M. Roland [1*] *and R. Casalini* [1,2]

[1]Chemistry Division, Code 6120, Naval Research Laboratory, Washington, DC 20375-5342, USA
[2]George Mason University, Chemistry Department, Fairfax, VA 22030, USA

We employ temperature modulated DSC (TMDSC) to determine the dependence of the fictive temperature on cooling rate for a series of polychlorinated biphenyls (PCB). From the slopes of semi-logarithmic plots of cooling rate *vs*. fictive temperature, the latter normalized by the fictive temperature for an arbitrary cooling rate, we determine the enthalpic fragilities. Despite significant differences in glass transition temperature and chemical structure (specifically chlorine content), the PCB have the same fragility. The value of the fragility determined using TMDSC is consistent with the fragility previously determined using dielectric relaxation spectroscopy.

Keywords: *chlorinated biphenyl, fragility, glass transition, PCB, TMDSC*

Introduction

A useful characteristic in assessing the vitrification behavior of glass-forming liquids and polymers is the fragility, *m*, which refers to the steepness of semi-logarithmic plots of the viscosity or structural relaxation time (or for polymers, the local segmental relaxation time) *vs.* T_g/T [1–4]. In such an analysis, the glass transition temperature, T_g, is commonly taken to be the temperature at which the relaxation time assumes some arbitrary long value, e.g., 100 s. In addition to being a useful metric of temperature sensitivity, the fragility is of interest because of its correlation to other properties of the material, such as the breadth of the relaxation function [5], the chemical structure [6–9], diffusion properties in the super-cooled regime [10, 11], Poisson's ratio of the glass [12], vibrational motions [13], Brillouin scattering intensities [14, 15] and even to nonlinear behavior in the glassy state [16, 17].

Although fragilities are usually determined from relaxation measurements (e.g., as

$$\left.\frac{d\log\tau}{d(T_g/T)}\right|_{T=T_g}$$

where τ is the dielectric or mechanical relaxation time), the kinetics of the glass transition, as influenced by the departure from equilibrium during cooling, can be related to the local relaxation dynamics and hence to fragility [18]. Upon cooling through T_g, the enthalpy departs from its equilibrium value, with the nonequilibrium state identified by its fictive temperature, T_f. The fictive temperature is defined as the temperature at which the nonequilibrium glass would be in equilibrium [19–21]. The degree of departure from equilibrium, and hence T_f, depend on the rate of cooling, q_c. Thus, the variation of the fictive temperature, determined from the heat capacity measured during heating following cooling at various rates, can be used to define an enthalpic fragility. Past work, using conventional DSC, has shown good correspondence between enthalpic and relaxation measures of fragilities [22–24]. More recently, TMDSC has been used to study the glass transition [25–27], and in particular Carpentier *et al.* used MDSC to measure enthalpic fragilities [28, 29]. In their method, the frequency of the temperature oscillation was varied with the consequent change in T_g used to calculate fragility. Thus, this application of MDSC is similar to alternating current calorimetry, as developed by Birge and Nagel [30, 31]. A drawback to the MDSC method of Carpentier *et al.* is that the frequency range is limited to about one decade, due to the requirement for sufficient data sampling over a period of the temperature oscillation [29].

In the present work we utilize MDSC to determine enthalpic fragilities from the dependence of the fictive temperature on cooling rate. Thus, a fixed oscillation frequency is used, and the dynamic range of the method is governed by the range of accessible cooling rates. This can routinely extend to 2 decades. The experiments were carried out on a series of polychlorinated biphenyls (PCB), varying in chlorine

* Author for correspondence: roland@nrl.navy.mil

1388–6150/$20.00

Akadémiai Kiadó, Budapest, Hungary
Springer, Dordrecht, The Netherlands

content. PCB are congener and isomer mixtures, with T_g determined by the average chlorine content. Especially intriguing is that the fragility, as determined by dielectric spectroscopy at atmospheric pressure, is the same for PCB having chlorine contents ranging from 42 to 62 mass% [32]. The presence of polar, bulky chlorine atoms would be expected to increase intermolecular cooperativity, and hence increase the fragility [9]. Thus, we use TMDSC to determine enthalpic fragilities on three PCB, and compare these values to the results from relaxation measurements.

Experimental

Samples employed herein were polychlorinated biphenyls (Monsanto Aroclors), obtained from J. Schrag of the University of Wisconsin. The samples are designated by their mass-average chlorine content, PCB42, PCB54 and PCB62.

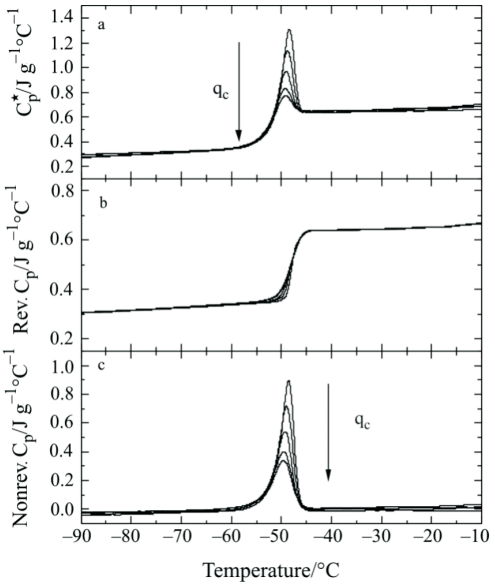

Fig. 1 a – Total heat capacity for PCB42, measured during heating at 2°C min^{-1}, following cooling at the rates q_c=5, 2, 0.5, 0.2 and 0.1°C min^{-1}; b – reversing component of the heat capacity, along with the fits to Eq.(1) in the glassy and liquid states; c – nonreversing heat flow curves, which exhibit a peak whose intensity is a measure of the structural recovery

TMDSC was carried out using a TA Instruments Q100, using liquid nitrogen cooling. Samples were cooled from the liquid state to 50°C below T_g, at rates, q_c, from 0.1 to 10°C min^{-1}. After 5 min, this was followed by heating at 2°C min^{-1} through T_g. The temperature modulation was ±0.5°C, with a 40 s period. The absolute value of the heat capacity was obtained after calibration using a synthetic sapphire [33].

Results

In Fig. 1 are displayed representative TMDSC data for PCB42. The curve for the total heat capacity (Fig. 1a) shows the usual overshoot due to enthalpy recovery. This kinetic component is isolated in the nonreversing heat capacity curve (Fig. 1c), whose peak reflects the degree of departure from equilibrium during the cooling. Integration of this peak yields an area used to calculate the fictive temperature. With decreasing cooling rate, there is a larger overshoot in the total heat flow curve, and a corresponding increase in the peak of the nonreversing heat flow. The reversing heat capacity is essentially invariant to q_c.

From the reversing heat flow curve in Fig. 1b, we calculate the heat capacity for the glass and the equilibrium liquid. Over the range of temperature measured herein (ca. 50°C on either side of T_g), both the glassy and liquid heat capacity can be represented by a linear function of temperature

$$C_p = a + bT \quad (1)$$

with the best-fit parameters for the three PCB given in Table 1. To determine the (cooling-rate dependent) fictive temperatures, we construct a parallelogram, having vertical sides defined by the respective glassy and liquid C_p. The boundary on the high temperature side is defined by the inflection of the reversing heat flow curve. This quantity is the common T_g, determined by conventional DSC; its value is given in Table 1 for a cooling rate equal to 2°C min^{-1}.

Figure 2 illustrates the method for obtaining T_f, as the location of the low temperature side of the parallelogram, such that the area is equal of the peak in the corresponding non-reversing heat flow curve. Obviously, $T_f < T_g$, except for the liquid in equilibrium,

Table 1 Glass transition temperature, fictive temperature, fits of the reversing heat capacity data, and fragility determined for the three PCB

Sample	T_g/K	T_f^*/K	C_P (liquid)		C_P (glass)		m
			$a^{\#}$/J g^{-1} K^{-1}	$b^{\#}$/J g^{-1} K^{-2}	$a^{\#}$/J g^{-1} K^{-1}	$b^{\#}$/J g^{-1} K^{-2}	
PCB42	225.1	217.5	0.664	$6.1\cdot10^{-4}$	0.409	$1.19\cdot10^{-3}$	74.3±6.4
PCB54	252.7	245.0	0.610	$5.4\cdot10^{-5}$	0.409	$1.41\cdot10^{-3}$	80.2±7.3
PCB62	274.3	265.0	0.273	$6.3\cdot10^{-4}$	$6.37\cdot10^{-2}$	$1.46\cdot10^{-3}$	78.2±3.2

*q_c=2°C min^{-1}; $^{\#}$equation 1

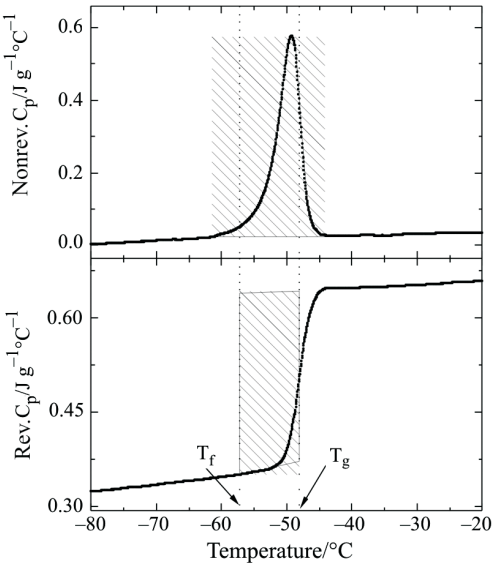

Fig. 2 Reversing heat capacity curve (lower panel) for PCB42 during heating at 2°C min^{-1}, following cooling at q_c=0.5°C min^{-1}, to depict the method used to calculate the fictive temperature, T_g is taken as the inflection point, while T_f is defined from the parallelogram having an area equal to the integral intensity of the peak in the nonreversing heat capacity curve (upper panel)

for which the fictive temperature becomes the glass transition temperature.

The dependence of the fictive temperature on cooling rate yields an apparent activation enthalpy for structural recovery [18]. The slope of semi-logarithmic plots of q_c as a function of the inverse fictive temperature normalized by a reference temperature defines an enthalpic fragility, $m \equiv -(d \log q_c)/[d(T_{f,ref}/T_f)]$. For the reference temperature, $T_{f,ref}$, we use the fictive temperature measured for q_c = 2°C min^{-1}. This is a relatively slow cooling rate, corresponding to a larger value of the structural recovery time. Results for the three PCB are displayed in Fig. 3. Over the range of the measurements (two decades of cooling rate), the data are roughly linear; that is, m is not a function of temperature (although it is a function of $T_{f,ref}$). The obtained m are given in Table 1. We find that within the experimental error, the fragility is independent of the chlorine content of the PCB, m=78±6. Dielectric spectroscopy results on these same PCB have been reported, and similarly m is the same for the different PCB [32, 34]. In the same fashion that the enthalpic fragility varies with $q_{c,ref}$, the relaxation measures of m depend on the value of the relaxation time used to define the reference temperature. Using $T_{f,ref}(\tau=100$ s), dielectric spectroscopy yields m=63 [32], while $T_{f,ref}(\tau=10$ s) gives m=58 [34]. The larger value of m as measured by MDSC reflects the fact that the structural recovery time for q_c=2°C min^{-1} is longer than 100 s. (Note that various 'rules of thumb' have been proposed; e.g., 2°C min^{-1}=38 s [16] and 10°C min^{-1}=100 s [3]). If we use data for a higher cooling rate to define $T_{f,ref}$ q_c=5°C min^{-1}, m decreases from 78 to 69. Higher cooling rates, necessary to more closely match the dielectric data, lack sufficient precision for a reliable determination of m.

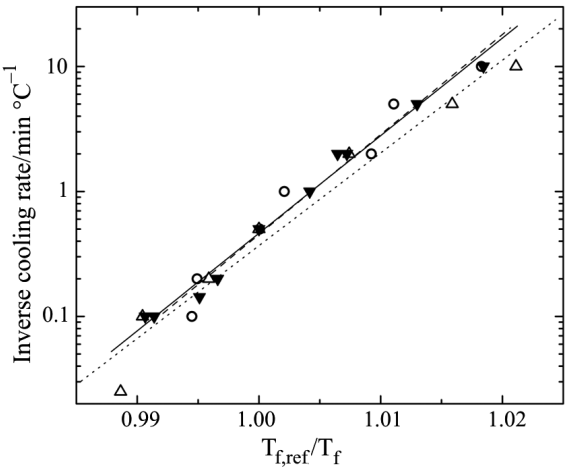

Fig. 3 Inverse cooling rate as a function of inverse fictive temperature normalized by T_f for q_c=2°C min^{-1}: ····△— PCB42, – – –○– PCB54 and – ▼ – PCB62 . The slopes yield the fragilities listed in Table 1

Conclusions

MDSC provides a facile means to determine the fragility, one of the important characteristics of the supercooled dynamics of glass-forming liquids. In conventional DSC experiments, the equilibrium heat flow is convoluted with the enthalpy recovery. MDSC avoids this problem, allowing the fictive temperature to be determined in a more straightforward manner. In this study, we found that for polychlorinated biphenyls, the fragility extracted from the enthalpy kinetics is consistent with determinations from dielectric relaxation spectroscopy. The unusual feature of the PCB is that their fragility is independent of chlorine content. This invariance of the fragility is consistent with the equivalence of the relaxation functions for the PCB [32], but surprising given the expected connection between chemical structure and relaxation properties [9]. This lack of correlation between molecular structure and fragility arises from the fact that the latter metric reflects both volume (density) and temperature contributions. As we have recently showed, especially for non-polymeric glass-formers, such as PCB, volume exerts a strong influence on the dynamics [35, 36]. Moreover, a recent investigation found that the contribution of volume to the glass transition dynamics increases with increasing chlorine content of PCB [34, 37]. It is only when the isochoric fragility is

considered does a correlation with chemical structure become apparent. This suggests that if the enthalpic fragility were determined from isochoric heat capacity measurements (i.e., C_V), differences in the behavior of the various PCB could be observed. It would be of interest therefore to measure DSC or TMDSC for these materials under elevated pressure.

Acknowledgements

This work was supported by the Office of Naval Research.

References

1 W. Oldekop, Glastech. Ber., 30 (1957) 8.
2 W. T. Laughlin and D. R. Uhlmann, J. Phys. Chem., 76 (1972) 2317.
3 C. A. Angell, J. Non-Cryst. Solids, 131–133 (1991) 13.
4 C. A. Angell, Science, 267 (1995) 1924.
5 R. Bohmer, K. L. Ngai, C. A. Angell and D. J. Plazek, J. Chem. Phys., 99 (1993) 4201.
6 C. M. Roland, Macromolecules, 27 (1994) 4242.
7 C. M. Roland and K. L. Ngai, Macromolecules, 24 (1991) 5315; 25 (1992) 1844.
8 C. M. Roland, Macromolecules, 25 (1992) 7031.
9 K. L. Ngai and C. M. Roland, Macromolecules, 26 (1993) 6824.
10 C. A. Angell, P. H. Poole and J. Shao, Nuovo Cimento, 16 (1994) 883.
11 C. M. Roland and K. L. Ngai, J. Chem. Phys., 104 (1996) 2967.
12 V. N. Novikov and A. P. Solkolov, Nature, 431 (2004) 961.
13 C. A. Angell, Polymer, 38 (1997) 6261.
14 T. Scopigno, G. Ruocco, F. Sette and G. Monaco, Science, 302 (2003) 849.
15 U. Buchenau and A. Wischnewski, Phys. Rev. B, 70 (2004) 092201.
16 I. M. Hodge, J. Non-Cryst. Solids, 203 (1996) 164.
17 C. M. Roland and K. L. Ngai, J. Non-Cryst. Solids, 212 (1997) 74.
18 I. M. Hodge, J. Non-Cryst. Solids, 169 (1994) 211.
19 A. Q. Tool, J. Am. Ceram. Soc., 29 (1946) 240.
20 A. Q. Tool, J. Res. Natl. Bur. Stand., 37 (1946) 73.
21 J. M. Hutchinson, Prog. Polym. Sci., 20 (1995) 703.
22 C. G. Robertson, P. G. Santangelo and C. M. Roland, J. Non-Cryst. Solids, 275 (2000) 153.
23 L. M. Wang, V. Velikov and C. A. Angell, J. Chem. Phys., 117 (2002) 10184.
24 C. M. Roland, P. G. Santangelo, C. G. Robertson and K. L. Ngai, J. Chem. Phys., 118 (2003) 10351.
25 J. F. Willart, M. Descamps and J. C. van Miltenburg, J. Therm. Anal. Cal., 51 (1998) 943.
26 L. Carpentier, L. Bourgeois and M. Descamps, J. Therm. Anal. Cal., 68 (2002) 727.
27 J. F. Masson, S. Bundalo-Perc and A. Delgado, J. Polym. Sci. Polym. Phys. Ed., 43 (2005) 276.
28 L. Carpentier, O. Bustin and M. Descamps, J. Phys. D Appl. Phys., 35 (2002) 402.
29 L. Carpentier, R. Decressain and M. Descamps, J. Chem. Phys., 121 (2004) 6470.
30 N. O. Birge and S. R. Nagel, Phys. Rev. Lett., 54 (1985) 2674.
31 N. O. Birge and S. R. Nagel, Rev. Sci. Instr., 58 (1987) 1464.
32 R. Casalini and C. M. Roland, Phys. Rev. B, 66 (2002) 180201.
33 D. A. Ditmars, S. Ishihara, S. S. Chang, G. Bernstein and E. D. West, J. Res. Nat. Bur. Stand., 87 (1982) 159.
34 C. M. Roland and R. Casalini, J. Chem. Phys., 122 (2005) 134505.
35 M. Paluch, R. Casalini and C. M. Roland, Phys. Rev. B, 66 (2002) 092202.
36 C. M. Roland, M. Paluch, T. Pakula and R. Casalini, Phil. Mag. B, 84 (2004) 1573.
37 R. Casalini and C. M. Roland, Phys. Rev. B, 71 (2005) 014210.

DOI: 10.1007/s10973-005-7221-7